2018 European Control Conference (ECC)
June 12-15, 2018. Limassol, Cyprus

Numerical simulations of two-dimensional neural fields with applications to working memory

Pedro M. Lima[1] and Wolfram Erlhagen[2]

Abstract— **In this paper we describe a neural field model which explains how a population of cortical neurons may encode in its firing pattern simultaneously the nature and time of sequential stimulus events. From the mathematical point of view, this is obtained my means of a two-dimensional field, where one dimension represents the nature of the event (for example the color of a light signal) and the other represents the elapsed time. Some numerical experiments are reported which were carried out using a computational algorithm for two-dimensional neural field equations. These numerical experiments are described and their results are discussed.**

I. INTRODUCTION

Dynamic Neural Fields (DNFs) have been introduced in the 1970s as simplified mathematical models of pattern formation in neural tissue in which the interaction of billions of neurons is treated as a continuum [19], [1]. These models take the form of nonlinear integro-differential equations on a spatially extended domain in which the integral kernel represents the spatial distribution of synaptic weights between neurons. Dynamic field theory is still a very active area of multidisciplinary research since the rich variety of spatiotemporal patterns that DNF models may generate are thought to be linked to various cognitive processes in the brain (for recent overviews see [4] and [16]). For this reason, there is an increased interest of the robotics community to apply the processing mechanisms offered by DNF for the development of brain-inspired control architectures. DNF have been first introduced into the domain of robotics in navigaton tasks to endow the attractor dynamis approach with memory and decision (see for example [2]). The approach has been later extended to human-robot interaction tasks with the goal to endow the robot with human-like social competences like imitation learning, action understanding and goal inference (see [6]). The self-sustaining properties of the neuronal population dynamics governed by DNF allow the system to cope with missing sensory information (e.g. due to occlusion) and to anticipate the action outcomes ahead of their realization. Moreover, the capacity to organize a sequence of behaviours is fundamental for a robot that is supposed to efficiently work in human environments. In [7] a DNF-based model is introduced that allows the robot to rapidly learn and memorize short sequences of sensorimotor events.

A specific example of application of DNF to robotics is working memory defined as the capacity to transiently hold sensory information to guide forthcoming action. DNF models with a kernel of lateral inhibition type support a spatially localized activity pattern, or "bump", that is initially triggered by an external stimulus. The activity remains self-sustained after stimulus removal due to the recurrent interactions in the network. In typical applications of one-dimensional (1D) field models, the neurons represent continuous stimulus dimensions such as position, color or tone pitch [17], [6]. The bump position thus defines a specific memorized value along the coded dimension. The mathematical analysis of a stimulus-specific bump [1] can be extended to derive rigorous conditions for the existence and stability of multibump solutions representing the memory of a series of transient inputs [8].

There have been few studies thus far that generalize mathematical results about bump solutions to two-dimensional (2D) fields (e.g., [11]). Conditions for the existence of symmetric 2D bumps have been derived [18]. Later work has shown that non-radially symmetric perturbations can destabilize bumps to a rich set of possible patterns existing in 2D fields [3].

The influence of noise in the dynamic behaviour of neural fields can be very important. This effect can be studied by means of stochastic versions of the neural field equations. The effect of additive noise is studied for example in [10]. In [9] the authors analyse the effect noise on bump solutions of neural fields. In the present paper we don't have place to discuss this important topic, therefore we focus only on the deterministic model.

We also remark that we consider here a mean field model, which does not consider explicitly the propagation of cortical waves. In this sense our approach differs significantly from detailed biophysical models used in the description of the cortex.

In this paper we investigate with the memory application in mind a numerical model that simulates how a sequence of inputs can generate a stable multibump solution in a 2D field. The study is motivated by recent neurophysiological findings suggesting that populations of cortical neurons may encode in their firing pattern simultaneously the nature and the timing (or temporal order) of sequential stimulus events [14]. The inputs to the field may be for example light signals of different colours that occur at different times. In this case,

*This work was supported by Portuguese National Fund (*Fundação para a Ciência e a Tecnologia*) within projects SFRH/BSAB/135130/2017 and UID/MAT/00013/2013

[1]The first author is with CEMAT (Center for Computational and Stochastic Mathematics), Instituto Superior Técnico, Universidade de Lisboa, Av. Rovisco Pais 1, 1049-001 LISBOA, Portugal plima@math.ist.utl.pt

[2]The second author is with CMAT (Center of Mathematics), Universidade do Minho, Campus Azurm Guimares, Portugal, wolfram.erlhagen@math.uminho.pt

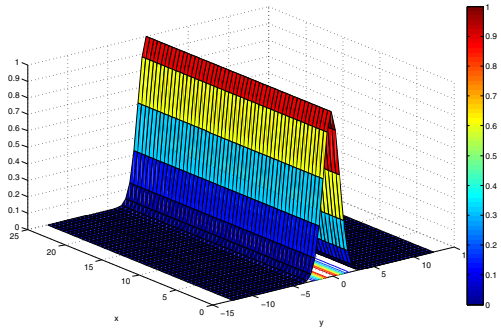

Fig. 1. Surface graph of the input function corresponding to a light signal of the color $y = 0$

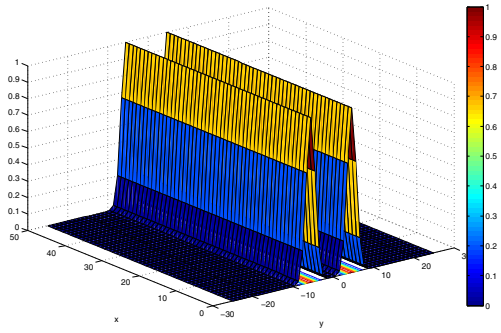

Fig. 2. Surface graph of the input function corresponding to light signals of colors $y_1 = -5$ and $y_2 = 5$

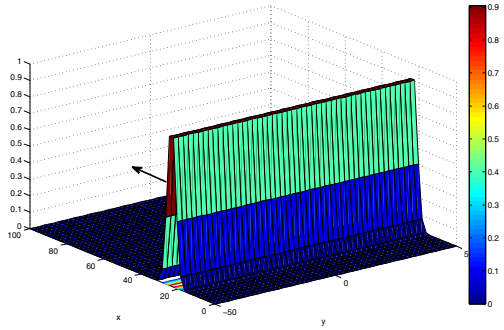

Fig. 3. Surface graph of the input function corresponding to a traveling wave, moving in the direction of the x axis

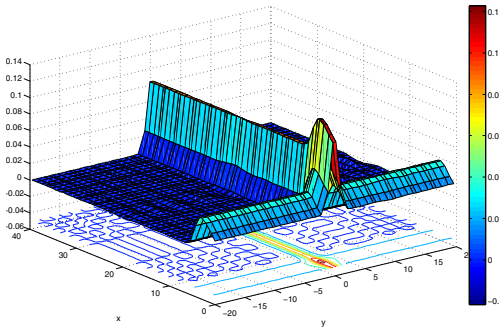

Fig. 4. Combination of two inputs generating a bump state

the field is spanned over the continuous dimensions colour (y-axis) and elapsed time (x-axis). The peak coordinates of a 2D bump contain respectively the information about the colour and the time interval of a specific event. A projection of the bump on the x and y axes reveals bell-shaped activity profiles which is consistent with the notion of broadly tuned neurons in the feature (colour) dimension and the time dimension [5], [14]. The localized activity pattern evolves from a low-activity resting state under the influence of two excitatory input sources. If a signal of colour y occurs at a certain time, we have a ridge-like input which is localized in the feature space y but extends in the time dimension x, see fig. 1. If several light signals of different colours occur simultaneously, the graphic of the input has several parallel ridges, whose coordinates $y_1, y_2, ...$ correspond to the different colours (see fig. 2).

Note that these inputs are transient, that is, they remain during a short time period and then vanish. The second input to the field is a traveling wave in form of a ridge which extends in y direction and propagates in the direction of x with elapsed time t since sequence onset at $t = 0$ (see [15] for a possible neural substrate). The graph of such input is displayed in fig.3.

Importantly, we assume that only at field positions which receive both inputs simultaneously, the combined input is strong enough to generate a transition from a stable resting state to the bump state (see fig.4) which persists after all inputs are switched off (see fig.5).

The structure of the rest of this paper is as follows. In Section 2 we give the mathematical formulation of the problem and the outline of the numerical algorithm. Some numerical examples are described in Section 3 and we finish with some conclusions in Section 4.

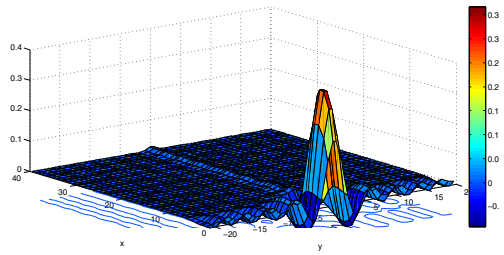

Fig. 5. Example of a stable bump solution which remains after all the inputs are switched off

II. Mathematical Formulation and Numerical Algorithm

We consider the Neural Field Equation in the form

$$c\frac{\partial}{\partial t}V(x,y,t) = I(x,y,t) - V(x,y,t) + \int_\Omega W(\|(x,y)-(x',y')\|_2)S(V(x',y',t))dx'dy', \quad t\in[0,T],(x,y)\in\Omega\subset I\!R^2, \tag{1}$$

where $V(x,y,t)$ represents the potential corresponding to the event (x,y) at instant t. The coordinates of the event are the and colour x and time y. Let us assume that $\Omega = [0,2L]\times[-L,L]$. The connectivity kernel W is of oscillating type:

$$W(r) = A\exp(-kr)\left(k\sin(a_1 r)+\cos(a_1 r)\right), \tag{2}$$

where A, a_1, k are certain positive constants (see [7]).

The activation function S is of Heavyside type:

$$S(V) = H(V-b),$$

where $b>0$ is a certain threshold.

I represents the sum of the external inputs and has several components:

$$I(x,y,t) = \sum_{i=0}^{n} I_i(x,y,t),$$

where I_0 is a traveling wave:

$$I_0(x,y,t) = \alpha_0\exp(-\gamma_0(x-vt)^2), \tag{3}$$

$0\le t\le T$, $(x,y)\in[0,2L]\times[-L,L]$, $v>0$ is a positive number: the remaining inputs are localized (peaks with center at C_i):

$$I_i(x,y,t) = \alpha_i\exp\left(-\gamma_i(y-C_i)^2\right), \tag{4}$$

where $C_i\in[-L,L]$, α_i,γ_i, are given positive numbers, $i=0,...,n$.

As initial condition we take

$$V(x,y,0)\equiv 0.$$

The numerical solution of this kind of two-dimensional problems is a challenge for computational methods. The choice of a sufficiently small discretization step size increases the cost of the spatial convolution. Moreover, we have to take into consideration that robot applications require *real time* performance, which imposes very strict constraints to the computing time. In this context, the efficiency of the numerical methods is of crucial importance. The computations presented here were carried out using an algorithm described in [13], which combines a second order implicit method for the time discretization with Gaussian quadrature rules for the integration in space. In the two-dimensional case, the required computational effort to solve equation (1) grows very fast as the discretization step is reduced, and therefore special attention has to be paid to the creation of effective methods. An important approach are the low-rank methods, as those discussed in [20], when the kernel is approximated by polynomial interpolation, which enables a significant reduction of the matrix dimensions. If for example the domain Ω is discretized by a mesh with 100×100 points, the low-rank method allows us (without loosing precision) to compute the solution only at $n\times n$ Chebyshev nodes, were n is in the range $10-20$, depending on the type of inputs considered in the specific problem.

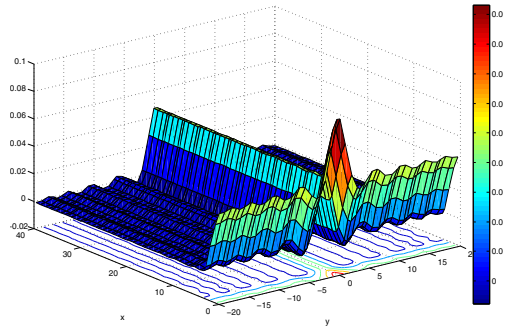

Fig. 6. Surface graphs of the solution at time $t=0.5$ in the case of Example 1

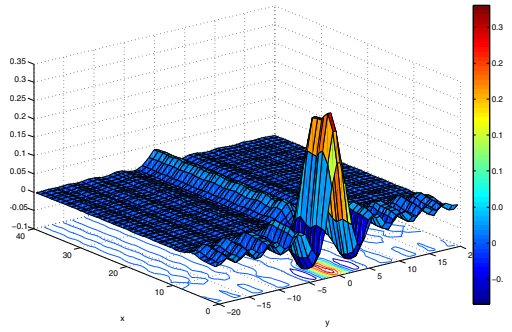

Fig. 7. Surface graphs of the solution at time $t=2.5$ in the case of Example 1

III. Numerical Examples

Example 1. In this example, the external input consists of a travelling wave I_0, described by (3), and a localized signal I_1, of the type (4), which are constant during the time interval $t\in[0,1.5]$ and then vanish. The corresponding parameters are: $\alpha_0=0.1$, $\gamma_0=1$, $v=5$; $\alpha_1=0.1$, $\gamma_1=1$, $C_1=0$. The threshold for the activation function is $b=0.1$; the connectivity kernel is described by (2), with the constants $A=0.02, k=0.8, a_1=1$. The domain of discretization is $[0,40]\times[-20,20]$; the step in time is $\tau=0.1$, the total number of time steps is $n_t=50$; the number of Chebyshev nodes is 25×25 and the number of gridpoints is 48×48.

In this case we observe that the combination of I_0 with I_1 generates at certain points a transition to the bump state (see fig. 6). When the potential at these points reaches the threshold $b=0.1$, an activity region arises, which remains as a one-bump solution after the external input is removed. (see fig. 7).

Example 2. In this case we have again a traveling wave I_0

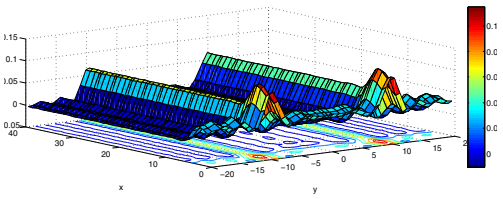

Fig. 8. Surface graphs of the solution at time $t = 1$ in the case of Example 2

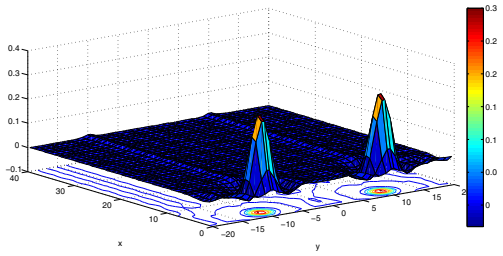

Fig. 9. Surface graphs of the solution at time $t = 5$ in the case of Example 2

and two localized inputs I_1 and I_2, with $\alpha_1 = 0.1$, $\gamma_1 = 1$, $C_1 = -10$ and $\alpha_2 = 1$, $\gamma_2 = 1$, $C_2 = 10$, which corresponds to an event with two different colors (see fig. 8). As in the previous example, inputs I_0, I_1 and I_2 are constant in the time interval $0 < t < 1$, and then are removed. All the other parameters have the same values as in previous example. We observe again an activity region which remains in the form of a two-bump solution after the input is removed (see fig.9).

We remark that in this figure the bumps have approximately the form of conic peaks, while in the previous example the bump was extended in the direction of x-axis (see fig. 7). This happens because the duration of the stimulus in Example 2 ($0 < t < 1$) is shorter than in the case of Example 1 ($0 < t < 1.5$). In this way, we observe that the output field also retains information about the duration of the stimulus.

Example 3. In this example, we have three series of inputs at different times. First in the time interval $[0, 1]$ we have I_0, I_1 and I_2 (with the same parameters as in Example 2); then on $[1, 3]$ we have only the traveling wave I_0; finally on $[3, 4]$ we have again I_0, I_1 and I_2. After $t = 4$ all the inputs are removed.

The output field of this example consists of a four-bump solution: two peaks correspond to the two first localized signals, and the remaining two ones correspond to the second series of signals.

The graphs describing the evolution of the output field in this case are displayed in fig. 10,11 and 12.

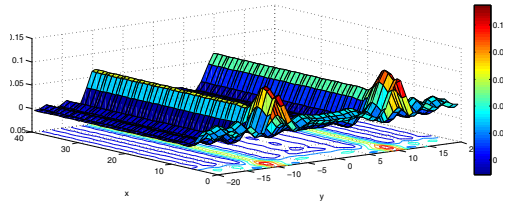

Fig. 10. Surface graphs of the solution at time $t = 1$ in the case of Example 3; here the output field contains only the representation of the first series of signals

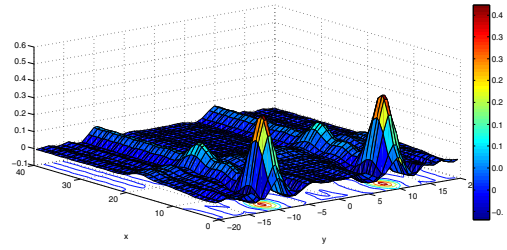

Fig. 11. Surface graphs of the solution at time $t = 4$ in the case of Example 3; at this moment we can see also a representation of the second series of signals.

Example 4. In this example, like in the preceeding one, we have three series of inputs at different times. First in the time interval $[0, 1.5]$ we have I_0 and I_1, where I_0 has the same parameters as in previous examples and I_1 is a localized signal of the form (4), with $\alpha_1 = 0.1$, $\gamma_1 = 1$, $C_1 = -10$; then on $[1.5, 3]$ we have only the travelling wave I_0; finally on $[3, 4.5]$ we have I_0, I_1 and I_2, where I_1 is described above and I_2 is a localized signal of the form (4), with $\alpha_2 = 0.1$, $\gamma_2 = 1$, $C_2 = 10$. After $t = 4.5$ all the inputs are removed.

The output field of this example consists of a three-bump

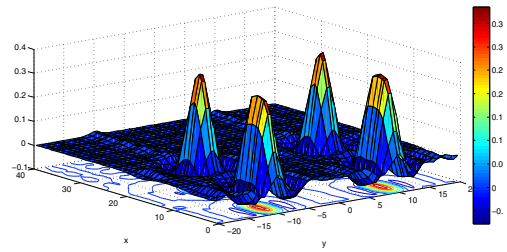

Fig. 12. Surface graphs of the solution at time $t = 7$ in the case of Example 3. Here we can see the stable four-bump field which remains after all the inputs are switched off.

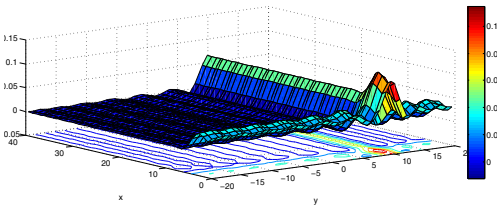

Fig. 13. Surface graphs of the solution at time $t = 1$ in the case of Example 4; the output field reflects the first signal.

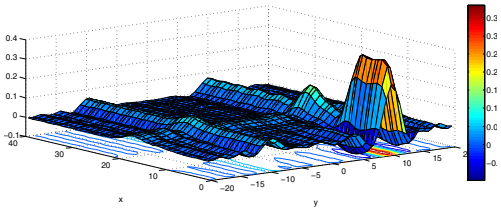

Fig. 14. Surface graphs of the solution at time $t = 4$ in the case of Example 4; at this time the output field also reflects the second series of signals.

solution: one peak corresponds to the first localized signal, and the remaining two ones correspond to the second series of signals.

The evolution of the output field for this example can be observed in figs. 13, 14 and 15. Graphs of the solution at different times show how the solution changes under the effect of the transient inputs and how a stable three-bump solution remains after all the inputs are switched off.

The numerical algorithm described above was coded in MATLAB. The computations were carried out in a PC with a 1.7Ghz processor, using 8 Gb of RAM. In such conditions each time step of the algorithm is performed in 5-9 sec, depending on the example.

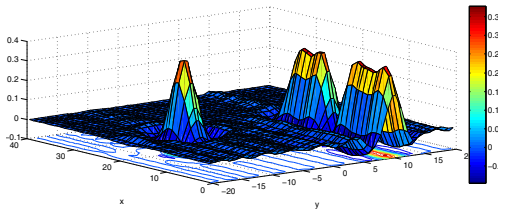

Fig. 15. Surface graphs of the solution at time $t = 7$ in the case of Example 4. Here we can see the stable three-bump field which remains after all the inputs are switched off.

IV. Conclusion

We have described a two-dimensional neural field model which explains how a population of cortical neurons may encode in its self-sustained firing pattern simultaneously the nature and time of sequential stimulus events [14]. Following the same neural processing mechanism, the memorized information can be recalled in a "read-out" field which receives the multibump pattern and the traveling wave I_0 as subthreshold inputs. As an important contribution to experimental and theoretical neuroscience, the postulated wave mechanism explains how a nervous system lacking specific sensors for temporal perception may develop neurons that respond to specific interval durations. Very recent findings in cell populations of rats performing timing tasks seem to support this computational mechanism [15].

A series of numerical experiments has been carried out, using a computational algorithm described in [13] for the numerical solution of the two-dimensional neural field equation (1).

The numerical results presented in section 3 actually support the conjecture that if the external input has appropriate intensity and duration, and if the connection kernel is of the type described by (2), the neural activity can generate stable multibump solutions which contain the information carried by the external signals. The results complement earlier numerical studies showing the formation of 2D multibump patterns which are solely defined by initial conditions [11].

For real world applications like for instance in robotics [6], the computing time is of critical importance. Though the computational algorithm used for these numerical experiments was designed to solve efficiently two-dimensional neural field equations, it was conceived to be used in a more general context and it may be not sufficiently fast to use in such applications. A possible way of improving this algorithm is to adapt it to the solution of problems of the class considered here, by taking advantage of some simplifications that can be done, when the problem data have the specific form described in Section 2. This is a direction of research that we intend to implement in the near future.

References

[1] S.L. Amari, "Dynamics of pattern formation in lateral-inhibition type neural fields", Biol. Cybernet., vol. 27 (2), pp. 77–87, 1977.

[2] E. Bicho and G. Schoener, "The dynamic approach to autonomous robotics demonstrated in a low-level vehicle platform", Robotics and Autonomous Systems, 21 (1), pp. 23-35, 1997.

[3] P. C. Bressloff, " Spatiotemporal dynamics of continuum neural fields", Journal of Physics A: Mathematical and Theoretical, vol. 45(3), pp. 033001, 2011.

[4] S. Coombes, P. Graben, R. Potthast, J. Wright, Neural Fields - Theory and Applications, Springer, 2014.

[5] W. Erlhagen et al., "The distribution of neuronal population activation (DPA) as a tool to study interaction and integration in cortical representations", Journal of neuroscience methods, vol. 94, vol. 1, pp. 53–66, 1999.

[6] W. Erlhagen and E. Bicho, "The dynamic neural field approach to cognitive robotics", Journal of Neural Engineering, vol. 3 (3), pp. R36, 2006.

[7] F. Ferreira, " Multi-bump solutions in dynamic neural fields: analysis and applications", PhD thesis, University of Minho, 2014 *http://hdl.handle.net/1822/34416*.

[8] F. Ferreira, W. Erlhagen, E. Bicho, "Multi-bump solutions in a neural field model with external inputs", Physica D: Nonlinear Phenomena, vol. 326, pp. 32–51, 2016.
[9] Z. Kilpatrick and B. Ermentrout, "Wandering bumps in stochastic neural fields",SIAM J. Appl. Dyn. Syst., vol. 12, pp. 61–94, 2013.
[10] C. Kühn and M.G. Riedler, "Large deviations for nonlocal stochastic neural fields"', J. Math. Neurosci, vol. 4, pp. 1–33 ,2014.
[11] C. R. Laing , W. C. Troy, B. Gutkin, and G.B. Ermentrout, "Multiple bumps in a neuronal model of working memory", SIAM Journal on Applied Mathematics, vol. 63 (1), pp.62–97, 2002.
[12] C. R. Laing and W. C. Troy, "PDE methods for nonlocal models", SIAM J. Appl. Dyn. Syst., vol. 22(3), pp. 487-516, 2006.
[13] P. M. Lima and E. Buckwar, "Numerical solution of the neural field equation in the two-dimensional case", SIAM J. Sci. Comput., vol. 37, pp. B962– B979, 2015.
[14] Mechant et al., "Interval tuning in the primate medial premotor cortex as a general timing mechanism", The Journal of Neuroscience, vol. 22, pp. 9082–9096, 2013.
[15] Mello et al., "A scalable population code for time in the striatum", Current Biology, vol. 25, pp.1113–1122, 2015.
[16] G. Schoener, J.P. Spencer et al., Dynamic Thinking a Primer on Dynamic Field Theory, Oxford University Press, 2016.
[17] A. Schutte, J. P. Spencer, and G. Schöner, "Testing the dynamic field theory: Working memory for locations becomes more spatially precise over development", Child Development, vol. 74 (5), pp. 1393–1417, 2003.
[18] H. Werner and R. Tim, "Circular stationary solutions in two-dimensional neural fields", vol. 85 (3), pp. 211–217, 2001.
[19] H.R. Wilson and J.D. Cowan, "Excitatory and inhibitory interactions in localized populations of model neurons", Bipophys. J., vol. 12, pp.1-24, 1972.
[20] Weng-Jing Xie and Fu-Rong Lin, "A fast numerical solution method for two dimensional Fredholm integral equations of the second kind", Applied Numerical Mathematics, vol. 59, pp. 1709-1719, 2009.